

Accurate stationary densities with partitioned numerical methods for stochastic partial differential equations

Kevin Burrage · Grant Lythe

Received: 23 April 2013 / Published online: 29 May 2014
© Springer Science+Business Media New York 2014

Abstract We consider the numerical solution, by finite differences, of second-order-in-time stochastic partial differential equations (SPDEs) in one space dimension. New timestepping methods are introduced by generalising recently-introduced methods for second-order-in-time stochastic differential equations to multidimensional systems. These stochastic methods, based on leapfrog and Runge–Kutta methods, are designed to give good approximations to the stationary variances and the correlations in the position and velocity variables. In particular, we introduce the reverse leapfrog method and stochastic Runge–Kutta Leapfrog methods, analyse their performance applied to linear SPDEs and perform numerical experiments to examine their accuracy applied to a type of nonlinear SPDE.

Keywords Stationary density · Stochastic Runge–Kutta methods · Leapfrog methods · Correlation function

Mathematics Subject Classification 65L06 · 60H15 · 60H35

K. Burrage
Department of Mathematics, Queensland University of Technology,
Brisbane, QLD 4001, Australia

K. Burrage
Department of Computer Science, University of Oxford, Oxford OX13QD, England

G. Lythe (✉)
Department of Applied Mathematics, University of Leeds, Leeds LS2 9JT, England
e-mail: grant@maths.leeds.ac.uk

1 Introduction

The dynamics of stochastic systems that are second order in time depends on the damping parameter, η . As $\eta \rightarrow 0$, the system exhibits properties similar to those of Hamiltonian systems. As $\eta \rightarrow \infty$, the system behaves similar to one that is first order in time. With the correct scaling of noise intensity, however, the stationary density is independent of η . In the case of scalar second order stochastic differential equations with additive noise and a damping term, it is possible to design numerical methods [8, 37, 38, 43, 45] with some desirable properties, described below, in all ranges of values of η [7]. While the analysis of these methods was given only in the linear case, these properties were shown to hold numerically for nonlinear problems as well. In this paper, we consider how to extend these ideas to second-order-in-time Stochastic Partial Differential Equations (SPDEs) in one space dimension with additive space-time white noise.

In one-degree-of-freedom linear systems, it is possible to devise timestepping methods with one Gaussian random variable per timestep, that have no systematic error in the position variable, and with a simple expression for the error in the velocity variable as a function of Δt [8]. New methods obtained from the analysis of linear equations were observed to perform well when applied to nonlinear systems [6]; whether they cope better with underdamped or overdamped systems, or equally-well with any value of damping, can be understood from the dependence of the error in linear systems on η . We shall follow this methodology here, producing timestepping methods for solution of systems of stochastic differential equations, using one Gaussian random variable per degree of freedom per timestep, from analysis of corresponding linear systems.

We shall consider the following second-order-in-time SPDE, known as ϕ^4 or Allen-Cahn [5, 11, 15, 20, 27, 29], that exhibits coherent structures called kinks:

$$\frac{\partial^2}{\partial t^2} \phi_t(x) + \eta \frac{\partial}{\partial t} \phi_t(x) = \frac{\partial^2}{\partial x^2} \phi_t(x) + f(\phi_t(x)) + (2\eta\Theta)^{\frac{1}{2}} \xi_t(x), \tag{1}$$

with periodic boundary conditions on $[0, l]$. The last term in (1) is space-time white noise:

$$\mathbb{E}(\xi_t(x)\xi_{t'}(x')) = \delta(x - x')\delta(t - t').$$

A configuration is a continuous function of x , $\phi_t(x)$, obtained by fixing t in one realization. At most values of x , $\phi_t(x)$ is close to either -1 or $+1$. A narrow region where the configuration crosses through 0 from below is called a kink; one where it crosses from above is called an antikink. In our scaling, the width of a kink is order 1 and the spatial domain is $[0, l]$; it is also possible to scale the width of a kink to ϵ on the spatial domain $[0, 1]$ [20, 22, 40]. Systematic computational studies of the SPDE require low temperatures in order to unambiguously identify kinks [15, 29]; they are computationally costly because the steady-state density of kinks decreases exponentially with temperature (so that l must be large) and the equilibration time increases exponentially with temperature.

After a sufficiently long time, in both the continuum SPDEs and the discrete system, a statistically-steady state is attained and maintained by a balance between con-

tinual nucleation of new domains and the diffusion and annihilation of existing ones [4, 9, 10, 15, 26, 30]. Many steady-state quantities, such as the mean number of kinks per unit length, can be calculated from the invariant density of the SPDE, by evaluating the partition function [3, 36, 39]. Further insight has recently been obtained by demonstrating the equivalence between the invariant density of paths of the SPDE, on the spatial domain, and the density of paths of a suitable bridge process [35, 41, 46].

2 Numerical solution

Consider the numerical solution of (1) in one space dimension [18, 19, 21, 24, 33, 34, 44]. We are interested in the correlation functions

$$c_q(x) = \lim_{t \rightarrow \infty} \mathbb{E}(\phi_t(x_0)\phi_t(x_0 + x)) \quad \text{and} \quad c_p(x) = \lim_{t \rightarrow \infty} \mathbb{E} \left(\frac{\partial \phi_t}{\partial t}(x_0) \frac{\partial \phi_t}{\partial t}(x_0 + x) \right).$$

Note that $c_q(x)$ and $c_p(x)$ are independent of x_0 and symmetric functions of x , taken modulo $[0, l]$. In a numerical solution, $c_q(x)$ and $c_p(x)$ are measured by choosing one or more x_0 and recording numerical means over a long realisation.

The numerical solution of the SPDE (1), using the finite-difference approximation, gives, via the Method of Lines applied to the spatial operator and the Brownian sheet, a set of N coupled stochastic differential equations [5, 13, 14]:

$$\begin{aligned} d\mathbf{X}_t &= I_N \mathbf{V}_t dt \\ d\mathbf{V}_t &= -\eta I_N \mathbf{V}_t dt + I_N f(\mathbf{X}_t) dt + k C_N \mathbf{X}_t dt + \epsilon d\mathbf{W}_t, \end{aligned} \tag{2}$$

where \mathbf{X}_t and \mathbf{V}_t are \mathbb{R}^N -valued random variables, written as $N \times 1$ column vectors, I_N is the N -dimensional identity matrix and $\mathbf{W} = (\mathbf{W}(1), \dots, \mathbf{W}(N))^T$, a column vector of N independent Wiener processes. The parameters k , N , and ϵ are related to Δx , l and Θ by

$$k = \Delta x^{-2}, \quad N = \frac{l}{\Delta x} \quad \text{and} \quad \epsilon^2 = \frac{2\eta\Theta}{\Delta x}.$$

The $N \times N$ symmetric matrix C_N is the discretised Laplacian

$$C_N = \begin{pmatrix} -2 & 1 & 0 & \dots & & 1 \\ 1 & -2 & 1 & 0 & \dots & \\ 0 & 1 & -2 & 1 & & \\ & & & \ddots & & \\ 0 & & \dots & 1 & -2 & 1 \\ 1 & 0 & \dots & & 1 & -2 \end{pmatrix}.$$

The limit $N \rightarrow 0$ corresponds to the SPDE limit $\Delta x \rightarrow 0$. We typically use values of N of order 10^5 . At finite Δx , the sets of random variables

$$\mathbf{X}_t = \begin{pmatrix} \mathbf{X}_t(1) \\ \vdots \\ \mathbf{X}_t(N) \end{pmatrix} \quad \text{and} \quad \mathbf{V}_t = \begin{pmatrix} \mathbf{V}_t(1) \\ \vdots \\ \mathbf{V}_t(N) \end{pmatrix},$$

representing “position” and “velocity”, provide an approximation to $\phi_t(i \Delta x)$ and $\frac{\partial \phi_t}{\partial t}(i \Delta x)$, $i = 1, 2, \dots, N$. We shall study timestepping methods that produce approximate solutions of (2), seeking accurate correlation functions for all values of η .

This work can be viewed as the extension, to N degrees of freedom, of recent results for the one-degree-of-freedom case. There, we considered [7, 8] second-order differential equations of the form $\ddot{x} = f(x) - \eta \dot{x} + \epsilon \xi(t)$, representing the motion of a particle subject to deterministic forces $f(x)$ and random forcing $\xi(t)$, where $\mathbb{E}(\xi(t)\xi(t')) = \delta(t - t')$. The amplitude of the random forcing, ϵ , is related to the temperature Θ and damping coefficient η by the fluctuation-dissipation relation $\epsilon^2 = 2\eta K \Theta$, where K is Boltzman’s constant. The deterministic force defines a potential function $U(x)$ via $f(x) = -U'(x)$.

Motivating examples Our main example will be the case $f(x) = x - x^3$. The effects of finite difference approximation are most easily explained in the case of the velocity–velocity correlations, $c_p(x)$. In the exact solution of (2),

$$c_p(x) = \begin{cases} 0 & x \neq 0 \\ \frac{\Theta}{\Delta x} & x = 0. \end{cases} \tag{3}$$

As long as a stationary density exists, the form (3) does not depend on $f(x)$ and is exact even when $\Delta x \neq 0$.

In Fig. 1, numerically-compiled averages of the velocity correlation function are displayed at three values of x . Each dot is compiled from one numerical realisation, with $N = 4 \times 10^5$, by averaging over samples taken once per time interval at times up to $t = 4 \times 10^5$. The value of $c_p(0)$ obtained at finite Δt differs from the exact value; the Runge–Kutta Leapfrog method shows the best convergence properties (left panel). At finite Δt , similarly, numerical mean values $c_p(i \Delta x)$, $i = 1, 2, \dots$ are not, in general, zero. One property of the reverse leapfrog method is that $c_p(i \Delta x)$, $i = 2, \dots$ is zero for linear systems and close to zero for nonlinear systems (right panel). The method also has the best convergence properties in $c_q(x)$, but we postpone discussion of this to later sections. The goal of the analysis we present in Sect. 3 is to calculate the convergence properties of timestepping methods.

3 Partitioned Runge–Kutta methods for systems of SDEs

Exact results can be obtained for linear systems, which serve as a testing ground for general, nonlinear, systems. Accordingly, in this Section we consider N -degree-of-

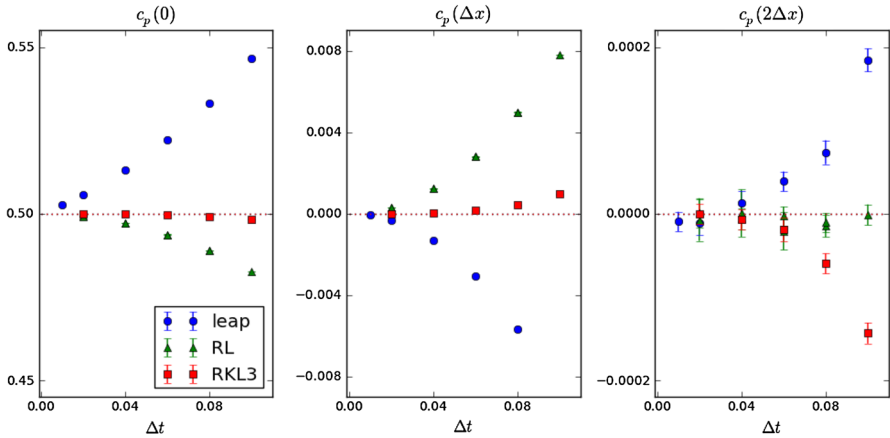


Fig. 1 Three numerical velocity–velocity correlations: the mean-square at one point in space, $c_p(0)$, the product at neighbouring sites, $c_p(\Delta x)$, and the product at a separation of two sites, $c_p(2\Delta x)$. The SPDE is solved using the leapfrog (leap), reverse leapfrog (RL) and three-stage Runge–Kutta leapfrog (RKL3) methods, with $\eta = 1.0$, $\theta = 0.2$ and $\Delta x = 0.4$. The exact results are shown as *dotted lines*

freedom linear systems described by

$$\begin{aligned} d\mathbf{X}_t &= I_N \mathbf{V}_t dt \\ d\mathbf{V}_t &= -\eta I_N \mathbf{V}_t dt - g I_N \mathbf{X}_t dt + k C_N \mathbf{X}_t dt + \epsilon d\mathbf{W}_t. \end{aligned} \tag{4}$$

Let

$$B_N = g I_N - k C_N,$$

then the set of SDEs (4) can be written as one matrix equation:

$$d \begin{pmatrix} \mathbf{X}_t \\ \mathbf{V}_t \end{pmatrix} = \begin{pmatrix} O_N & I_N \\ -B_N & -\eta I_N \end{pmatrix} \begin{pmatrix} \mathbf{X}_t \\ \mathbf{V}_t \end{pmatrix} dt + \epsilon \begin{pmatrix} O_N \\ I_N \end{pmatrix} d\mathbf{W}_t,$$

where O_N is the $N \times N$ zero matrix.

Our task is to examine how faithfully the stationary density is reproduced by standard and new timestepping methods for SPDEs. These methods produce approximate values for the positions and velocities at discrete times $t_n, n = 0, 1, 2, \dots$. We denote these values by $X_n(i)$ and $V_n(j), i, j = 1, \dots, N$. Usually $t_{n+1} - t_n$ is a fixed number Δt . We consider the evolution of X_n and V_n and their statistical properties as $t_n \rightarrow \infty$, and compare with the exact results

$$\lim_{t \rightarrow \infty} \mathbb{E}(\mathbf{X}_t^T \mathbf{X}_t) = \frac{\epsilon^2}{2\eta} L_N, \quad \lim_{t \rightarrow \infty} \mathbb{E}(\mathbf{X}_t^T \mathbf{V}_t) = O_N \quad \text{and} \quad \lim_{t \rightarrow \infty} \mathbb{E}(\mathbf{V}_t^T \mathbf{V}_t) = \frac{\epsilon^2}{2\eta} I_N,$$

where [17]

$$L_N = B_N^{-1}.$$

3.1 Partitioned Runge–Kutta methods

Let

$$q_n = \begin{pmatrix} X_n(1) \\ \vdots \\ X_n(N) \end{pmatrix} \quad \text{and} \quad p_n = \begin{pmatrix} V_n(1) \\ \vdots \\ V_n(N) \end{pmatrix}.$$

When solving (2) under a partitioned Runge–Kutta (PRK) method [25] with s stages, q_{n+1} and p_{n+1} are obtained from q_n and p_n via s intermediate vectors Y_i and Z_i :

$$p_{n+1} = p_n + \sum_{j=1}^s b_j(-\eta Z_j + f(Y_j) + kC_N Y_j)\Delta t + \epsilon \Delta W_n,$$

$$q_{n+1} = q_n + \sum_{j=1}^s \hat{b}_j Z_j \Delta t,$$

where $\Delta W_n = (\Delta W_n(1), \dots, \Delta W_n(N))^T$, and each $\Delta W_n(i)$ is drawn independently from a Gaussian distribution with mean zero and variance Δt . The intermediate vectors satisfy

$$Z_i = p_n + \sum_{j=1}^s a_{ij}(-\eta Z_j + f(Y_j) + kC_N Y_j)\Delta t + \epsilon c_i \Delta W_n$$

$$Y_i = q_n + \sum_{j=1}^s \hat{a}_{ij} Z_j \Delta t. \tag{5}$$

Note that N Gaussian random variables are required per timestep. We use the notation $e = (1, 1, \dots, 1)^T$, $b = (b_1, b_2, \dots, b_s)^T$, $\hat{b} = (\hat{b}_1, \hat{b}_2, \dots, \hat{b}_s)^T$, $c = (c_1, c_2, \dots, c_s)^T$ and let A and \hat{A} be the $s \times s$ matrices whose entries are the a_{ij} and \hat{a}_{ij} in (5). We assume $c = Ae$ and $b^T e = 1$, and represent PRK methods by pairs of Butcher tableaux [16]:

$$\left| \begin{array}{c} A \\ \hline b^T \end{array} \right| \quad \left| \begin{array}{c} \hat{A} \\ \hline \hat{b}^T \end{array} \right|.$$

Let $Z = (Z_1, Z_2, \dots, Z_s)^T$, $Y = (Y_1, Y_2, \dots, Y_s)^T$ and $f(Y) = (f(Y_1), f(Y_2), \dots, f(Y_s))^T$. Then we can write (5) as

$$\begin{aligned}
 (I_S \otimes I_N + \eta A \otimes I_N \Delta t)Z &= e \otimes p_n + (A \otimes I_N)f(Y)\Delta t + (A \otimes C_N)Yk\Delta t \\
 &\quad + \epsilon c \otimes \Delta W_n \\
 Y &= e \otimes q_n + (\hat{A} \otimes I_N)Z\Delta t.
 \end{aligned}
 \tag{6}$$

If a PRK method is applied to the linear system, $f(Y) = -gY$, then (6) simplifies to

$$\begin{aligned}
 PZ &= e \otimes p_n - (c \otimes B_N)q_n\Delta t + \epsilon c \otimes \Delta W_n \\
 Y &= e \otimes q_n + \hat{A}Z\Delta t,
 \end{aligned}$$

where

$$P = I_S \otimes I_N + \eta A \otimes I_N \Delta t + (A\hat{A}) \otimes B_N \Delta t^2.
 \tag{7}$$

Thus

$$\begin{aligned}
 p_{n+1} &= p_n - \eta b^T \otimes I_N Z\Delta t - b^T \otimes B_N Y\Delta t + \epsilon \Delta W_n \\
 q_{n+1} &= q_n + \hat{b}^T \otimes I_N Z\Delta t
 \end{aligned}
 \tag{8}$$

and we can write

$$\begin{pmatrix} q_{n+1} \\ p_{n+1} \end{pmatrix} = R \otimes \begin{pmatrix} q_n \\ p_n \end{pmatrix} + \epsilon r \otimes \Delta W_n,
 \tag{9}$$

where

$$R = \begin{pmatrix} R_{11} & R_{12} \\ R_{21} & R_{22} \end{pmatrix} \quad \text{and} \quad r = \begin{pmatrix} R_1 \\ R_2 \end{pmatrix}.$$

Comparing (8) with (9), we find

$$\begin{aligned}
 R_{11} &= I_N - (\hat{b}^T \otimes I_N)P^{-1}(c \otimes B_N)\Delta t^2 \\
 R_{12} &= (\hat{b}^T \otimes I_N)P^{-1}(e \otimes I_N)\Delta t \\
 R_{21} &= - \left(I_N - \eta(b^T \otimes I_N)P^{-1}(c \otimes I_N)\Delta t + (b^T \hat{A} \otimes B_N)P^{-1}(c \otimes I_N)\Delta t^2 \right) B_N \Delta t \\
 R_{22} &= I_N - \eta(b^T \otimes I_N)P^{-1}(e \otimes I_N)\Delta t - (b^T \hat{A} \otimes B_N)P^{-1}(e \otimes I_N)\Delta t^2 \\
 R_1 &= (\hat{b}^T \otimes I_N)P^{-1}(c \otimes I_N)\Delta t \\
 R_2 &= I_N - \eta(b^T \otimes I_N)P^{-1}(c \otimes I_N)\Delta t - (b^T \hat{A} \otimes B_N)P^{-1}(c \otimes I_N)\Delta t^2.
 \end{aligned}$$

The R_{ij} , as well as R_1 and R_2 , are $N \times N$ symmetric matrices and functions of Δt .

Let

$$\Sigma_n = \mathbb{E} \left(\begin{pmatrix} q_n^T \\ p_n^T \end{pmatrix} \begin{pmatrix} q_n^T & p_n^T \end{pmatrix} \right).$$

The stationary density of the numerical method is characterised by $\Sigma = \lim_{n \rightarrow \infty} \Sigma_n$. We shall search for methods such that

$$\Sigma = \frac{\epsilon^2}{2\eta} \begin{pmatrix} L_N & O_N \\ O_N & J_N \end{pmatrix}.
 \tag{10}$$

Thus, while requiring exact statistics in the discretised positions, we describe the numerical error in the velocities in terms of the difference between J_N and the $N \times N$ identity as a function of Δt and η .

With a numerical update of the form (9), Σ_{n+1} is related to Σ_n by

$$\Sigma_{n+1} = R \Sigma_n R^T + \epsilon^2 \begin{pmatrix} R_1^T \\ R_2^T \end{pmatrix} \begin{pmatrix} R_1^T & R_2^T \end{pmatrix} \Delta t, \quad \text{where } R^T = \begin{pmatrix} R_{11}^T & R_{21}^T \\ R_{12}^T & R_{22}^T \end{pmatrix}.$$

The required form (10) of the stationary correlation matrix will be found if $S = 0$ where

$$S = R \begin{pmatrix} L_N & O_N \\ O_N & J_N \end{pmatrix} R^T - \begin{pmatrix} L_N & O_N \\ O_N & J_N \end{pmatrix} + 2\eta \begin{pmatrix} R_1 R_1^T & R_1 R_2^T \\ R_2 R_1^T & R_2 R_2^T \end{pmatrix}.$$

The condition $S = 0$ is equivalent to the following three equations:

$$\begin{aligned} R_{11} L_N R_{11} - L_N + R_{12} J_N R_{12} + 2\eta R_1 R_1 \Delta t &= 0 \\ R_{11} L_N R_{21} + R_{12} J_N R_{22} + 2\eta R_1 R_2 \Delta t &= 0 \\ R_{21} L_N R_{21} + R_{22} J_N R_{22} - J_N + 2\eta R_2 R_2 \Delta t &= 0. \end{aligned}$$

Notice that

$$\begin{aligned} R_1 B_N \Delta t &= I_N - R_{11} \\ R_2 B_N \Delta t &= -R_{21}. \end{aligned}$$

3.2 Basic result on systems

It is convenient to define

$$\begin{aligned} T_N &= (\hat{b}^T \otimes I_N) P^{-1} (c \otimes I_N) \\ U_N &= (\hat{b}^T \otimes I_N) P^{-1} (e \otimes I_N) \\ Z_N &= (\eta b^T \otimes I_N + \Delta t b \hat{A} \otimes B_N) P^{-1} (c \otimes I_N) \\ W_N &= (\eta b^T \otimes I_N + \Delta t b \hat{A} \otimes B_N) P^{-1} (e \otimes I_N), \end{aligned} \tag{11}$$

with P given by (7). Then

$$\begin{aligned} R_{11} &= I_N - T_N B_N \Delta t^2 & R_{12} &= U_N \Delta t \\ R_{21} &= -(I_N - Z_N \Delta t) B_N \Delta t & R_{22} &= I_N - W_N \Delta t \\ R_1 &= T_N \Delta t & R_2 &= I_N - Z_N \Delta t, \end{aligned}$$

and

$$-(T_N B_N L_N + L_N^T B_N T_N^T) + T_N^T B_N B_N^T T_N \Delta t^2 + U_N J_N U_N^T + 2\eta \Delta t^2 T T^T = 0.$$

Since $B_N = B_N^T, T_N = T_N^T, U_N = U_N^T$ and $B_n L_N = I_N$, we find

$$J_N = 2U_N^{-2}T_N \left(I_N - (\eta\Delta t + \frac{1}{2}B_N\Delta t^2)T_N \right). \tag{12}$$

That is, $J_N = \alpha(\eta I_N \Delta t, B_N \Delta t^2)$, where $\alpha(\eta \Delta t, g \Delta t^2)$ is the scalar function (1.19) in [8].

4 Timestepping methods for systems of SDEs

We now consider specific examples of timestepping methods, beginning with two-stage methods.

4.1 The implicit midpoint method

For reference, we give the Butcher tableaux and corresponding matrix P for the implicit midpoint method. The tableaux are

$$\begin{array}{c|cc} 0 & 0 & 0 \\ \frac{1}{2} & 0 & \frac{1}{2} \\ \hline & 0 & 1 \end{array},$$

and

$$P = \begin{pmatrix} I_N & O_N \\ O_N & I_N(1 + \frac{1}{2}\eta\Delta t) + \frac{1}{4}B_N\Delta t^2 \end{pmatrix}.$$

Thus

$$\begin{aligned} R_{11} &= \left(I_N + \frac{1}{2}\eta\Delta t I_N + \frac{1}{4}B_N\Delta t^2 \right)^{-1} \left(I_N + \frac{1}{2}\eta\Delta t I_N - \frac{1}{4}B_N\Delta t^2 \right) \\ R_{12} &= \left(I_N + \frac{1}{2}\eta\Delta t I_N + \frac{1}{4}B_N\Delta t^2 \right)^{-1} \Delta t \\ R_{21} &= \left(I_N + \frac{1}{2}\eta\Delta t I_N + \frac{1}{4}B_N\Delta t^2 \right)^{-1} B_N \Delta t \\ R_{22} &= \left(I_N + \frac{1}{2}\eta\Delta t I_N + \frac{1}{4}B_N\Delta t^2 \right)^{-1} \left(I_N - \frac{1}{2}\eta\Delta t I_N - \frac{1}{4}B_N\Delta t^2 \right). \end{aligned}$$

and there is no error in the velocity–velocity correlations [7,37,38]:

$$J_N = I_N.$$

However, this method is implicit and therefore not convenient for use on nonlinear systems.

4.2 The leapfrog method

The leapfrog method is represented in Butcher tableaux as:

$$\begin{array}{c|cc} 0 & 0 & 0 \\ 1 & 1 & 0 \\ \hline & 1 & 0 \end{array} \quad \begin{array}{c|c} 1/2 & 0 \\ 1/2 & 0 \\ \hline 1/2 & 1/2 \end{array},$$

which gives, after some simplification, $J_N = (I_N(1 - \frac{1}{2}\eta\Delta t) - \frac{1}{4}B_N\Delta t^2)^{-1}$, thus generalising the result of [7].

4.3 Mannella’s method

Mannella’s modification of the leapfrog method [31,32] is represented as:

$$\begin{array}{c|cc} 0 & 0 & 0 \\ 1 & 1/2 & 1/2 \\ \hline & 1/2 & 1/2 \end{array} \quad \begin{array}{c|c} 1/2 & 0 \\ 1/2 & 0 \\ \hline 1/2 & 1/2 \end{array};$$

it has $J_N = (I_N - \frac{1}{4}B_N\Delta t^2)^{-1}$. This is an improvement on the standard leapfrog method because $J_N - I_N$, the error in the velocity–velocity correlation function, is proportional to Δt^2 and independent of η .

4.4 The reverse leapfrog method

This is represented as

$$\begin{array}{c|cc} \frac{1}{2} & \frac{1}{2} & 0 \\ \frac{1}{2} & \frac{1}{2} & 0 \\ \hline & \frac{1}{2} & \frac{1}{2} \end{array} \quad \begin{array}{c|c} 0 & 0 \\ \frac{1}{2} & \frac{1}{2} \\ \hline \frac{1}{2} & \frac{1}{2} \end{array}.$$

As $A\hat{A} = 0$, we can show

$$P = \begin{pmatrix} (1 + \frac{1}{2}\eta\Delta t)I_N & O_N \\ \frac{1}{2}\eta\Delta t I_N & I_N \end{pmatrix}$$

and

$$R_{11} = I_N - \frac{1}{2} \frac{1}{1 + \frac{1}{2}\eta\Delta t} B_N \Delta t^2$$

$$R_{12} = \left(1 + \frac{1}{1 + \frac{1}{2}\eta\Delta t} \right) I_N \Delta t$$

$$R_{21} = \left(I_N - \frac{1}{2} \frac{\eta \Delta t}{1 + \frac{1}{2} \eta \Delta t} I_N + \frac{1}{2} \frac{\Delta t^2}{1 - \frac{1}{2} \eta \Delta t} B_N \right) B_N \Delta t^2$$

$$R_{22} = \frac{1 - \frac{1}{2} \eta \Delta t}{1 + \frac{1}{2} \eta \Delta t} I_N + \frac{1}{2} B_N \frac{\Delta t^2}{1 + \frac{1}{2} \eta \Delta t}.$$

This yields

$$J_N = I_N - \frac{1}{4} B_N \Delta t^2.$$

As with the Mannella method, the reverse leapfrog method is efficient and easily implemented and has the virtues of giving the exact correlation function in the positions variable, and an error in the velocity variables independent of η . In addition, the form of $J_N - I_N$ means that the correlations introduced in the velocity variable are only one Δx step on either side, since $B_N = g I_N - k C_N$.

The correlation introduced in the velocity variable is independent of η and only occurs between neighbouring grid points:

$$c_p(0) = 1 - \frac{1}{4} (2k + g) \Delta t^2, \quad c_p(\Delta x) = \frac{1}{4} k \Delta t^2 \quad \text{and} \quad c_p(i \Delta x) = 0, \text{ for } i > 1,$$

consistent with the results shown in Fig. 1.

4.5 Runge–Kutta leapfrog methods

In this section we give a more detailed analysis of the class of Runge–Kutta leapfrog methods introduced in [8]. We first introduce the simplifying assumptions that were made in that paper.

Theorem 1 *If the following conditions, known as property A, hold [8]:*

$$b^T = \hat{b}^T \quad b^T A = \frac{1}{2} b^T \quad A \hat{A} e = \frac{1}{2} c \quad b^T e = 1.$$

Then

$$U_N = I_N - (\eta \Delta t I_N + \frac{1}{2} \Delta t^2 B_N) T_N$$

and

$$J_N = 2 T_N U_N^{-1}.$$

Proof The formula for J_N is given by (11) and (12) with

$$J_N = 2 U_N^{-2} T_N \left(I_N - (\eta \Delta t + \frac{1}{2} B_N \Delta t^2) T_N \right),$$

where

$$\begin{aligned} T_N &= (\hat{b}^T \otimes I_N)P^{-1}(c \otimes I_N) \\ U_N &= (\hat{b}^T \otimes I_N)P^{-1}(e \otimes I_N) \\ P &= I_S \otimes I_N + A \otimes I_N \eta \Delta t + (A\hat{A}) \otimes B_N \Delta t^2. \end{aligned}$$

Expanding P^{-1} and repeatedly using Property A and $Ae = c$ gives

$$\begin{aligned} U_N &= I_N + \sum_{j=1}^{\infty} (-1)^j (b^T \otimes I_N)(A \otimes I_N \eta \Delta t + A\hat{A} \otimes B_N \Delta t^2)^{j-1} (c \otimes I_N \eta \Delta t \\ &\quad + \frac{1}{2}c \otimes B_N \Delta t^2) = I_N - (\eta \Delta t I_N + \frac{1}{2} \Delta t^2 B_N)T_N. \end{aligned}$$

Hence $J_N = 2T_N U_N^{-1}$. □

This is the generalisation, to N -degree-of-freedom systems, of Lemma 3.2 in [8]. There, the strategy was to construct classes of PRK methods with high order.

Runge–Kutta leapfrog methods with $s \geq 3$ stages and increasingly high order [8] are constructed as follows. In addition to property A, let

$$\hat{A} = \frac{1}{2}I - e_s v^T, \tag{13}$$

where v is chosen so that $v^T e = 0$ and $v^T = (v_1, v_2, \dots, \frac{1}{2})$ and with a value $k = s - 2$ such that

$$v^T A^{j-1} c = 0, \quad j = 1, \dots, k. \tag{14}$$

Let

$$X_N = \eta \Delta t I_N + \frac{1}{2} \Delta t^2 B_N$$

then (13) and (14) give

$$(b^T \otimes I_N)(A \otimes I_N \eta \Delta t + A\hat{A} \otimes B_N \Delta t^2)^j (c \otimes I_N) = b^T A^j c X_N^j \quad j = 1, \dots, k,$$

and

$$\begin{aligned} &(b^T \otimes I_N)(A \otimes I_N \eta \Delta t + A\hat{A} \otimes B_N \Delta t^2)^{k+1} (c \otimes I_N) \\ &= b^T A^{k+1} c X_N^{k+1} - (b^T A e_s)(v^T A^k c) \Delta t^2 B_N X_N^k \end{aligned}$$

so that

$$T_N = b^T c I_N + \sum_{j=1}^{k+1} (-1)^j (b^T A^j c) X_N^j + M_N + O(\Delta t^{k+3}),$$

where

$$M_N = (-1)^{k+2} (b^T A e_s) (v^T A^k c) \Delta t^2 B_N X_N^k.$$

Now, with property A,

$$b^T A^j c = \left(\frac{1}{2}\right)^{j+1}, \quad \forall j,$$

so

$$2T_N = I_N + \sum_{j=1}^{k+1} (-1)^j \left(\frac{1}{2}\right)^j X_N^j + 2M_N + O(\Delta t^{k+3}).$$

Thus from Theorem 4.1

$$2T_N = U_N + 2M_N + O(\Delta t^{k+3}).$$

Hence

$$\begin{aligned} J_N &= 2T_N U_N^{-1} \\ &= I_N + 2M_N U_N^{-1} + O(\Delta t^{k+3}), \end{aligned}$$

and so the error in J_N is

$$J_N - I_N = 2(-1)^{k+2} (b^T A e_s) (v^T A^k c) \Delta t^{k+2} \eta^k B_N.$$

and this is consistent with the scalar result first given in [8] where $k + 2 = s$. Thus the lowest-order correlations introduced into the velocity variable, proportional to B_N , are only one spatial step on either side.

4.6 $s = 3$

Example: The three-step Runge–Kutta leapfrog method, satisfying Property A, was first given in [6] and takes the form

$$\begin{aligned} Y_1 &= q_n + \frac{1}{2} \Delta t p_n \\ Z_2 &= \left(1 - \frac{1}{2} \eta \Delta t\right) p_n + \frac{1}{2} ((f(Y_1) + C_N Y_1) \Delta t + \epsilon \Delta W) \\ Y_2 &= q_n + \frac{1}{2} \Delta t Z_2 \\ Y_3 &= 2Y_2 - Y_1 \end{aligned}$$

$$\begin{aligned}
 p_{n+1} &= \frac{1}{1 + \frac{1}{2}\eta\Delta t} \\
 &\quad \left(\left(1 - \frac{1}{2}\eta\Delta t\right)p_n - \frac{1}{4} \left(f(Y_1) + 2f(Y_2) + f(Y_3) + C_N Y_2\right) \Delta t + \epsilon \Delta W \right) \\
 q_{n+1} &= q_n + \frac{1}{2}(p_n + p_{n+1}).
 \end{aligned}$$

We find

$$\begin{aligned}
 P &= \begin{pmatrix} I_N & O_N & O_N \\ \frac{1}{2}\eta\Delta t I_N + \frac{1}{4}\Delta t^2 B_N & I_N & O_N \\ -\frac{1}{2}\eta\Delta t I_N - \frac{1}{2}B_N \Delta t^2 & \eta\Delta t I_N + B_N \Delta t^2 & (1 + \frac{1}{2}\eta)I_N \end{pmatrix}, \\
 T_N &= \frac{1}{2}I_N - \frac{1}{4} \left(\eta\Delta t I_N + \frac{1}{2}B_N \Delta t^2\right) + \frac{1}{8} \left(\eta\Delta t I_N + \frac{1}{2}B_N \Delta t^2\right) \eta\Delta t I_N + \dots \\
 U_N &= I_N - \frac{1}{2} \left(\eta\Delta t I_N + \frac{1}{2}B_N \Delta t^2\right) + \frac{1}{4} \left(\eta\Delta t I_N + \frac{1}{2}B_N \Delta t^2\right)^2 + \dots \\
 J_N &= I_N - \frac{1}{8} \left(\eta\Delta t I_N + \frac{1}{2}B_N \Delta t^2\right)^2 + \frac{1}{4} \left(\eta\Delta t I_N + \frac{1}{2}B_N \Delta t^2\right) \eta\Delta t I_N + \dots \\
 &= I_N - \frac{1}{8}\eta\Delta t^3 B_N + \dots
 \end{aligned}$$

The error is proportional to $\eta\Delta t^3$, consistent with the one-degree-of-freedom case [8].

5 Timestepping methods for the ϕ^4 SPDE

We now return to our nonlinear example, the kink-bearing SPDE with $f(x) = -U'(x)$ where $U(x) = -\frac{1}{2}x^2 + \frac{1}{4}x^4$. Let us consider the functions $c_q(x)$ and $c_p(x)$ in the limit $\Delta x \rightarrow 0$. The nonlinearity of the SPDE does not affect the exact velocity correlation function, $c_p(x)$, which is still zero if $x \neq 0$. The steady state density of the field at a point is non-Gaussian with mean-square, $c_q(0)$, calculated as $\Delta x \rightarrow 0$ as follows. Let ϵ_n and $\psi_n(u)$ be the eigenvalues, and corresponding normalised eigenfunctions, of the equation [5, 12, 28]

$$\left(-\frac{1}{2\beta^2} \frac{\partial^2}{\partial u^2} + U(u) \right) \psi_n(u) = \epsilon_n \psi_n(u),$$

where $\beta = \Theta^{-1}$ and $n = 0$ corresponds to the eigenfunction with the smallest eigenvalue. Then

$$c_q(x) = \sum_n s_n^2 \exp(-\beta x(\epsilon_n - \epsilon_0)),$$

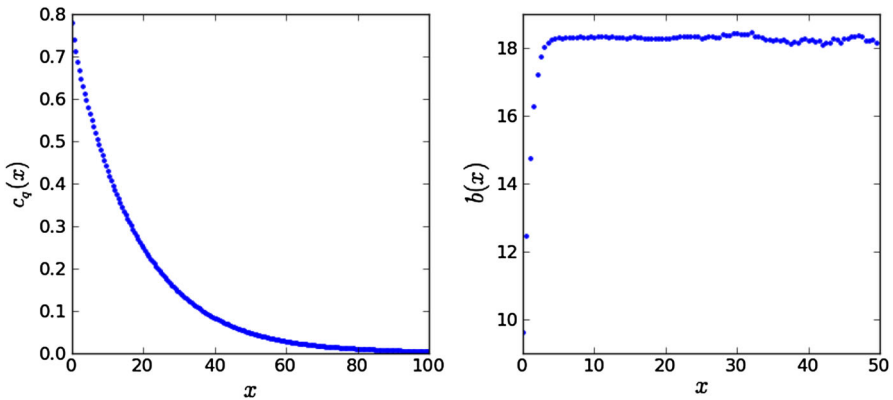


Fig. 2 The correlation function $c_q(x)$ and the corresponding $b(x)$ constructed from a numerical solution with $\beta = 5, k = 4, \eta = 1$

where $s_n = \int_{-\infty}^{\infty} u \psi_n(u) \psi_0(u) du$. The most important feature of the correlation function is the exponential term with exponent $\beta(\epsilon_1 - \epsilon_0)$, where ϵ_1 is the next-to-smallest eigenvalue: as $x \rightarrow \infty, c_q(x) \propto \exp(-x/\lambda)$, where $\lambda^{-1} = \beta(\epsilon_1 - \epsilon_0)$. To estimate λ from a numerical solution we plot the following function of x :

$$b(x) = \Delta x \left(\log \left(\frac{c_q(x)}{c_q(x + \Delta x)} \right) \right)^{-1},$$

so that $\lim_{x \rightarrow \infty} b(x) = \lambda$. The numerical $b(x)$ plateaus at the value λ (Figure 2). In our numerical runs, we used $N = 10^5$ grid points and averaged over samples taken every 10 time units up to time $t = 10^6$.

In Fig. 3, we compare the accuracy of $c_q(x), c_p(x)$ and λ , measured numerically. In the quantity that is the most challenging to measure numerically, λ , the reverse leapfrog method performs remarkably well. The Runge–Kutta leapfrog method, however, is most accurate in $c_p(\Delta x)$. Timestepping methods included in Fig. 3 are the standard leapfrog and Mannella’s modification [31,32], the Heun method, and the reverse leapfrog method, all of which are two-stage methods using one Gaussian random variable per timestep. Also shown is the three-stage Runge–Kutta leapfrog method [8]. The code used to produce these results is given as supplementary material, along with a code that produces an animated illustration of the dynamics and measurement of the density.

In Fig. 4, we compare the accuracy of $c_q(0)$ (the mean-square of ϕ , where there is still error associated with finite Δx even as $\Delta t \rightarrow 0$) and of $c_p(x)$ at three values of x and two values of η . The reverse leapfrog method performs best in the position variable (upper panel) and the velocity correlation function at a separation of two grid points (lower panel). However, the three-stage and four-stage Runge–Kutta leapfrog methods [8] are most accurate in the velocity correlation function at zero and one grid point separation. Methods with five or more stages can be implemented similarly.

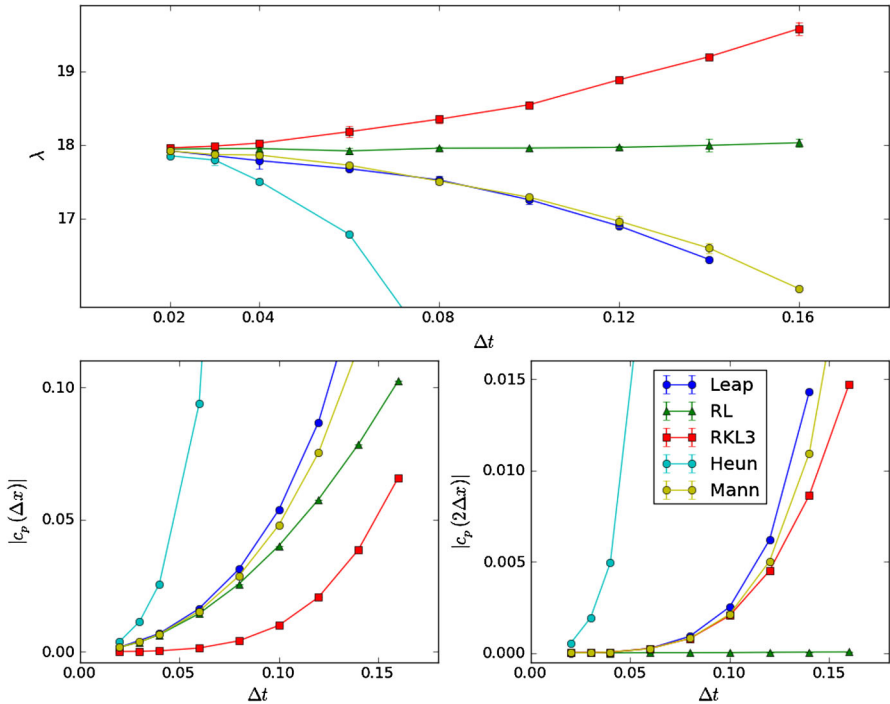


Fig. 3 Performance of different algorithms as a function of Δt . The values of $\beta = 5$, $\eta = 1.0$ and $\Delta x = 0.25$ are fixed. In the *upper graph*, the correlation length λ is shown as a function of Δt ; the reverse leapfrog method is most accurate. In the *lower left panel*, $|c_p(\Delta x)|$ is plotted; the most accurate algorithm is the third-order Runge–Kutta leapfrog method. In the *lower right panel*, $|c_p(2\Delta x)|$ is plotted; the error in this quantity with the reverse leapfrog method is smaller than the statistical error

6 Discussion

In this paper we have constructed classes of Runge–Kutta methods for solving second-order-in-time SPDEs in one space dimension based on the finite difference approximation. Two-stage methods are available that improve on the standard leapfrog method in important ways. A series of multistage methods, with increasing accuracy in the stationary density, have also been devised and implemented. These methods are essentially those described in [8]; here we show how they behave in multidimensional systems, yielding good accuracy in the stationary variances and the correlations in the position and velocity variables while using only one Wiener increment per step irrespective of the number of stages.

Numerical methods satisfying weak convergence criteria have been constructed recently [1, 23, 42]. The focus, usually on constructing higher order methods and methods with good linear stability properties, is also shifting towards consideration of methods that preserve the stationary density function [2]. However, our approach is still novel in its focus on second-order-in-time, or Langevin, dynamics.

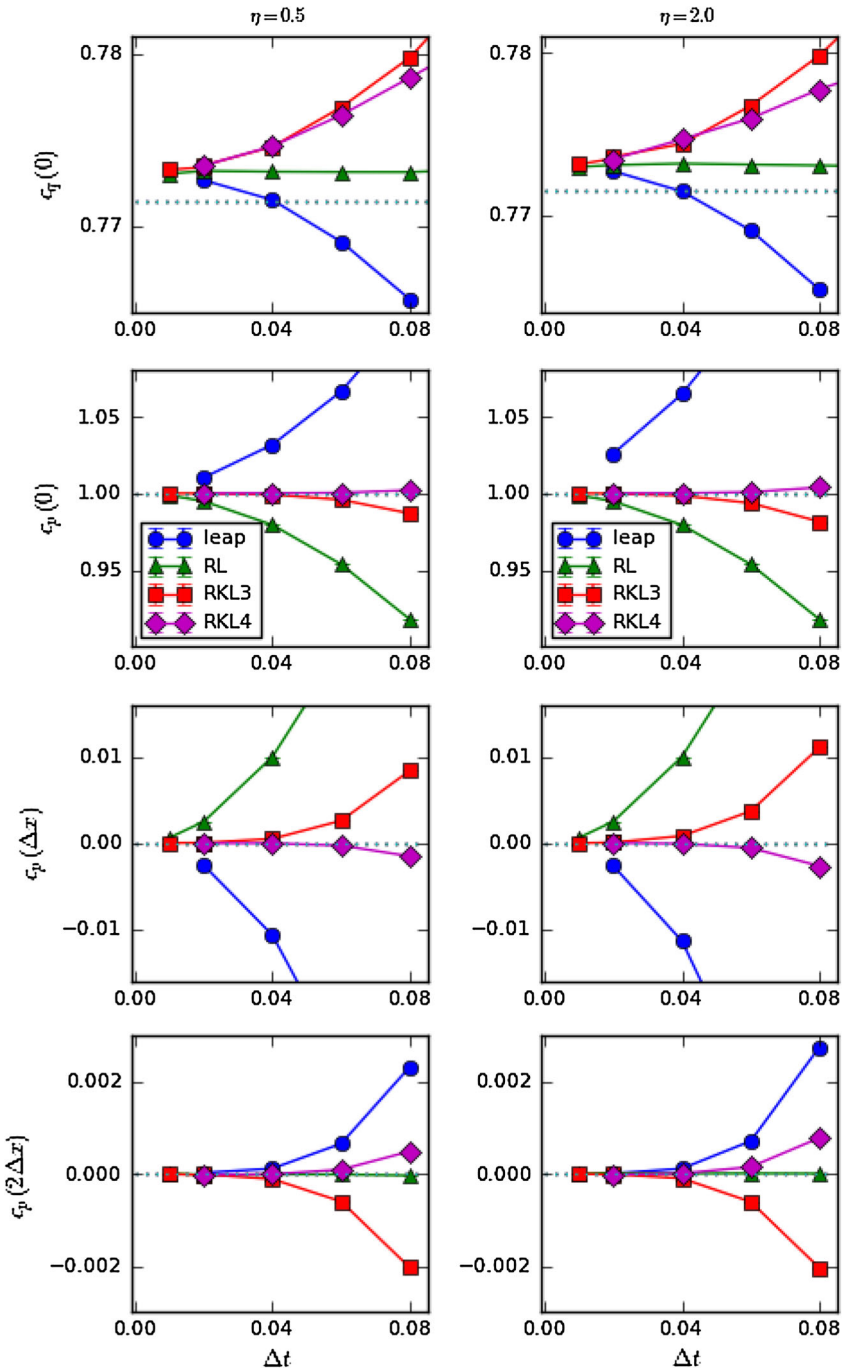


Fig. 4 Numerical means, as a function of Δt , with $\Delta x = 0.2$. *Left column* $c_p(0)$. *Central column* $c_p(0)$. *Right column* $c_p(\Delta x)$. *Top row* $\eta = 0.5$. *Bottom row* $\eta = 2.0$. The timestepping methods used are the standard leapfrog (leap), reverse leapfrog (RL), three-stage and four-stage Runge–Kutta leapfrog (RKL3 and RKL4). Exact continuum results are shown as *dotted lines*

A recent paper [6] considered the behaviour of Runge–Kutta methods applied to nonlinear Hamiltonian problems with additive noise, with an independent Wiener increment added per stage rather than per step. This approach is more expensive but it can be shown that it allows for better dynamic properties associated with the method and, in particular, for the midpoint rule this preserves the mean of the problem exactly at each step - this is not the case if just one Wiener process is used per step. We will consider the extension of this idea to examples considered in this paper in future work.

References

1. Abdulle, A., Cirilli, S.: S-ROCK: Chebyshev methods for stiff stochastic differential equations. *SIAM J. Sci. Comput.* **30**(2), 997–1014 (2008)
2. Abdulle, A., Vilmart, G., Zygalkakis, K. et al.: High order numerical approximation of the invariant measure of ergodic sdes. MATHICSE Technical Report Nr. 27.2013, EPFL, Lausanne, Switzerland (2013)
3. Alexander, F.J., Habib, S.: Statistical mechanics of kinks in 1+1 dimensions. *Phys. Rev. Lett.* **71**(7), 955–958 (1993). doi:[10.1103/PhysRevLett.71.955](https://doi.org/10.1103/PhysRevLett.71.955)
4. Berglund, N., Gentz, B.: Anomalous behavior of the Kramers rate at bifurcations in classical field theories. *J. Phys. A* **42**(5), 052001 (2009)
5. Bettencourt, L., Habib, S., Lythe, G.: Controlling one-dimensional Langevin dynamics on the lattice. *Phys. Rev. D* **60**, 105039–105047 (1999)
6. Burrage, K., Burrage, P.M.: Low rank Runge–Kutta methods, symplecticity and stochastic hamiltonian problems with additive noise. *J. Comput. Appl. Math.* **236**, 3920 (2012)
7. Burrage, K., Lenane, I., Lythe, G.: Numerical methods for second-order stochastic differential equations. *SIAM J. Sci. Comput.*, 29(1):245–264 (2007). doi:[10.1137/050646032](https://doi.org/10.1137/050646032). <http://link.aip.org/link/?SCE/29/245/1>
8. Burrage, K., Lythe, G.: Accurate stationary densities with partitioned numerical methods for stochastic differential equations. *SIAM J. Numer. Anal.* **47**, 1601–1618 (2009)
9. Büttiker, M., Christen, T.: Nucleation of weakly driven kinks. *Phys. Rev. Lett.* **75**, 1895–1898 (1995)
10. Büttiker, M., Landauer, R.: Nucleation theory of overdamped soliton motion. *Phys. Rev. Lett.* **43**, 1453–1456 (1979)
11. Castro, M., Lythe, G.: Numerical experiments on noisy chains: from collective transitions to nucleation-diffusion. *SIAM J. Appl. Dyn. Syst.*, 7(1):207–219 (2008). doi:[10.1137/070695514](https://doi.org/10.1137/070695514). <http://link.aip.org/link/?SJA/7/207/1>
12. Currie, J.F., Krumhansl, J.A., Bishop, A.R., Trullinger, S.E.: Statistical mechanics of one-dimensional solitary-wave-bearing scalar fields: exact results and ideal-gas phenomenology. *Phys. Rev. B* **22**, 477 (1980)
13. Gyongy, I.: Lattice approximations for stochastic quasi-linear parabolic partial differential equations driven by space-time white noise I. *Potential Anal.* **9**, 1–25 (1998)
14. Gyongy, I.: Lattice approximations for stochastic quasi-linear parabolic partial differential equations driven by space-time white noise II. *Potential Anal.* **11**, 1–37 (1999)
15. Habib, S., Lythe, G.: Dynamics of kinks: nucleation, diffusion and annihilation. *Phys. Rev. Lett.* **84**, 1070–1073 (2000)
16. Hairer, E., Norsett, S.P., Wanner, G.: *Solving Ordinary Differential Equations I: Nonstiff Problems*. Springer, Berlin (1993)
17. Hairer, M., Stuart, A.M., Voss, J., Wiberg, P.: Analysis of SPDEs arising in path sampling. Part I: the Gaussian case. *Commun. Math. Sci.* **3**, 587–603 (2005)
18. Jentzen, A., Peter, E.K.: Overcoming the order barrier in the numerical approximation of stochastic partial differential equations with additive space-time noise. *Proc. R. Soc. A* **465**(21), 649–667 (2009)
19. Jentzen, A., Kloeden, P.E.: *Taylor approximations for stochastic partial differential equations*. SIAM, Philadelphia (2011)
20. Katsoulakis, M.A., Kossioris, G.T., Lakkis, O.: Noise regularization and computations for the 1-dimensional stochastic Allen–Cahn problem. *Interfaces Free Bound.* **9**, 1–30 (2007)

21. Kloeden, P.E., Lord, G.J., Neuenkirch, A., Shardlow, T.: The exponential integrator scheme for stochastic partial differential equations: pathwise error bounds. *J. Comput. Appl. Math.* **235**(5), 1245–1260 (2011)
22. Kohn, R.V., Otto, F., Reznikoff, M.G., Vanden-Eijnden, E.: Action minimization and sharp-interface limits for the stochastic Allen–Cahn equation. *Commun. Pure Appl. Math.* **LIX**, 0001–0046 (2006)
23. Komori, Y., Burrage, K.: Weak second order S-ROCK methods for Stratonovich stochastic differential equations. *J. Comput. Appl. Math.* **236**(11), 2895–2908 (2012)
24. Kunita, H.: *Stochastic Flows and Stochastic Differential Equations*. Cambridge University Press, Cambridge (1997)
25. Leimkuhler, B., Reich, S.: *Simulating Hamiltonian Dynamics*. Cambridge University Press, Cambridge (2004)
26. Lothe, J., Hirth, J.P.: Dislocation dynamics at low temperatures. *Phys. Rev.* **115**(3), 543–550 (1959). doi:[10.1103/PhysRev.115.543](https://doi.org/10.1103/PhysRev.115.543)
27. Lythe, Grant, Habib, Salman: Stochastic PDEs: convergence to the continuum? *Comput. Phys. Commun.* **142**, 29–35 (2001)
28. Lythe, G., Habib, S.: Kinks in a stochastic PDE. In N.Sri Namachchivaya and Y.K.Lin, editors, *Proceedings of the IUTAM symposium on Nonlinear Stochastic Dynamics*, pages 435–444. Kluwer (2003)
29. Lythe, G., Habib, S.: Kink stochastics. *Comput. Sci. Eng.* **8**(3), 10–15 (2006)
30. Maier, R.S., Stein, D.L.: Droplet nucleation and domain wall motion in a bounded interval. *Phys. Rev. Lett.* **87**(27), 270601 (2001)
31. Mannella, R.: Quasisymplectic integrators for stochastic differential equations. *Phys. Rev. E* **69**, 041107 (2004)
32. Mannella, R.: Numerical stochastic integration for quasi-symplectic flows. *SIAM J. Sci. Comput.* **27**, 2121–2139 (2006)
33. Da Prato, G., Zabczyk, J.: *Stoch. Equ. Infin. Dimens.* Cambridge University Press, Cambridge (1992)
34. Prévôt, C., Röckner, M.: *A Concise Course on Stochastic Partial Differential Equations*. Springer, Berlin (2007)
35. Reznikoff, M.G., Vanden-Eijnden, E.: Invariant measures of stochastic partial differential equations and conditioned diffusions. *Comptes Rendus Academy Sciences Paris* **1340**, 305–308 (2005)
36. Scalapino, D.J., Sears, M., Ferrell, R.A.: Statistical mechanics of one-dimensional Ginzburg–Landau fields. *Phys. Rev. B* **6**, 3409–3416 (1972)
37. Schurz, H.: Preservation of probabilistic laws through Euler methods for Ornstein–Uhlenbeck processes. *Stoch. Anal. Appl.* **17**, 463–486 (1999)
38. Schurz, H.: Numerical analysis of SDEs without tears. In: Kannan, D., Lakshmikantham, V. (eds.) *Handbook of Stochastic Analysis and Applications*, pp. 237–359. Marcel Dekker, New York (2002)
39. Seeger, A., Schiller, P.: Kinks in dislocation lines and their effects on the internal friction in crystals. In: Mason, W.P. (ed.) *Physical Acoustics: Principles and Methods*, pp. 361–495. Academic Press, New York (1966)
40. Shardlow, T.: Stochastic perturbations of the Allen–Cahn equation. *Electron. J. Differ. Equ.* **47**, 1–19 (2000)
41. Stuart, A.M., Voss, J., Wiberg, P.: Conditional path sampling of SDEs and the Langevin MCMC method. *Commun. Math. Sci.* **2**, 585–697 (2004)
42. Tretyakov, M.V., Zhang, Z.: A fundamental mean-square convergence theorem for SDEs with locally Lipschitz coefficients and its applications. *SIAM J. Numer. Anal.* **51**(6), 3135–3162 (2013)
43. Voss, J.: The effect of finite element discretisation on the stationary distribution of SPDEs. *Commun. Math. Sci.* **10**, 1143–1159 (2012)
44. Walsh, J.B.: An introduction to stochastic partial differential equations. In P.L.Hennequin, editor, *Ecole d’été de probabilités de St-Flour XIV*, pages 266–439 (1986)
45. Wang, W., Skeel, R.D.: Analysis of a few numerical integration methods for the Langevin equation. *Mol. Phys.* **101**, 2149 (2003)
46. Weber, Hendrik: Sharp interface limit for invariant measures of a stochastic Allen–Cahn equation. *Commun. Pure Appl. Math.* **63**(8), 1071–1109 (2010)